J. Phys. Chem. A **2009,** *113,* 2591–2599

Effect of a Heteroatom on Bonding Patterns and Triradical Stabilization Energies of 2,4,6-Tridehydropyridine versus 1,3,5-Tridehydrobenzene

Prashant U. Manohar, Lucas Koziol, and Anna I. Krylov*

Department of Chemistry, University of Southern California, Los Angeles, California 90089-0482

Received: November 30, 2008; Revised Manuscript Received: January 8, 2009

Electronic structure of 2,4,6-tridehydropyridine and isoelectronic 1,3,5-tridehydrobenzene is characterized by the equation-of-motion spin-flip coupled-cluster calculations with single and double substitutions and including perturbative triple corrections. Equilibrium geometries of the three lowest electronic states, vertical and adiabatic states ordering, and triradical stabilization energies are reported for both triradicals. In 1,3,5-tridehydrobenzene, the ground $^2A_1$ state is 0.016 eV below the $^2B_2$ state, whereas in 2,4,6-tridehydropyridine the heteroatom reverses adiabatic state ordering bringing $^2B_2$ below $^2A_1$ by 0.613 eV. The doublet−quartet gap is also larger in 2,4,6-tridehydropyridine as compared to 1,3,5-tridehydrobenzene; the respective adiabatic values are 1.223 and 0.277 eV. Moreover, the heteroatom reduces bonding interactions between the C_2 and C_6 radical centers, which results in the increased stabilizing interactions between C_4 and C_2/C_6. Triradical stabilization energies corresponding to the separation of C_4 and C_2 are 19.7 and −0.2 kcal/mol, respectively, in contrast to 2.8 kcal/mol in 1,3,5-tridehydrobenzene. Similarly weak interactions between C_2 and C_6 are also observed in 2,6-didehydropyridine resulting in a nearly zero singlet−triplet energy gap, in contrast to *m*-benzyne and 2,4-didehydropyridine. The total interaction energy of the three radical centers is very similar in 1,3,5-tridehydrobenzene and 2,4,6-tridehydropyridine and is 19.5 and 20.1 kcal/mol, respectively.

1. Introduction

Triradicals are highly reactive species characterized by the presence of three unpaired electrons in three near-degenerate orbitals.[1] Orbital near-degeneracies result in closely lying electronic states characterized by distinctly different bonding patterns between the unpaired electrons and, therefore, different chemical properties. In addition to their fundamental importance, triradicals also attract considerable attention due to their potential role as building blocks of organic magnets.[2−8]

Electronic near-degeneracies and multiconfigurational open-shell wave functions of triradicals pose a challenge to electronic structure methodology. Indeed, quantitative predictions of energy differences between the triradical states, which are important for the design of magnetic materials, require proper account of both dynamical and nondynamical correlation, as well as accurate equilibrium geometries. The equation-of-motion spin-flip (EOM-SF) approach[9−21] is an efficient and robust computational tool for studying triradicals. When implemented within coupled-cluster with single and double substitutions (CC) framework (EOM-SF-CCSD),[10,18] the method demonstrated[17] accuracy exceeding conservative estimate of EOM-EE-CCSD error bars (0.1−0.3 eV), and inclusion of triple excitations[20,21] brought the error bars below chemical accuracy (1 kcal/mol). Analytic gradients implemented for EOM-SF-CCSD[19] enable calculations of equilibrium geometries including both dynamical and nondynamical correlation.

The interactions between the unpaired electrons, which may range from strongly antibonding (repulsion) to almost a complete chemical bond, have distinct structural, spectroscopic, and chemical signatures. For example, bonding interactions result in shorter distances between the radical centers, more rigid structures (i.e., higher vibrational frequencies), and reduced reactivity. Energetically, these partial bonds can be quantified using triradical stabilization energy (TSE).[22] In analogy to the definition by Wierschke et al. of diradical stabilization energy (DSE),[23] TSE is defined as the enthalpy (at 0 K) of a hypothetical isodesmic reaction in which a radical center is transferred from a triradical to the corresponding closed-shell precursor yielding a diradical and a monoradical. Positive TSE indicates stabilization of the triradical relative to the separated radical centers. The reactions defining TSEs of 1,3,5-tridehydrobenzene (TDB) and 2,4,6-tridehydropyridine (TDP) are shown in Figure 1, and those defining related DSEs are shown in Figure 2. TSEs of all three tridehydrobenzene isomers, as well as DSEs of the parent benzynes, have been computed and analyzed in ref 24. The relatively low value of 2.8 kcal/mol

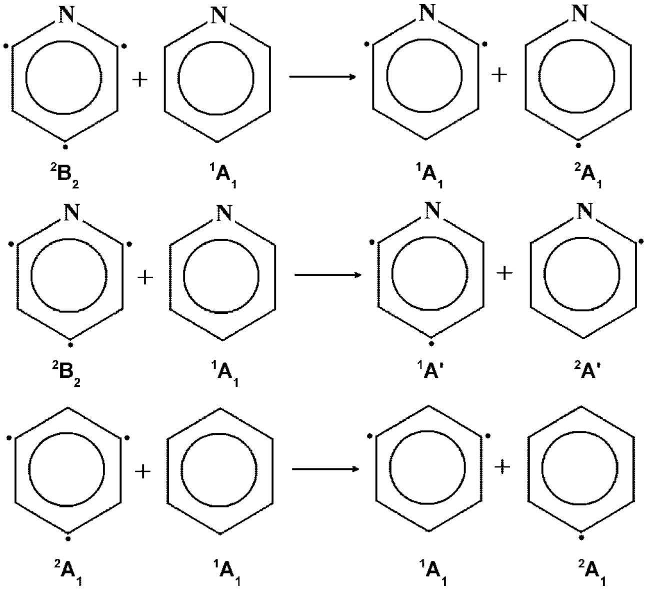

Figure 1. Pseudoisodesmic reactions defining triradical stabilization energies of 2,4,6-tridehydropyridine and 1,3,5-tridehydrobenzene.

10.1021/jp810522e CCC: $40.75

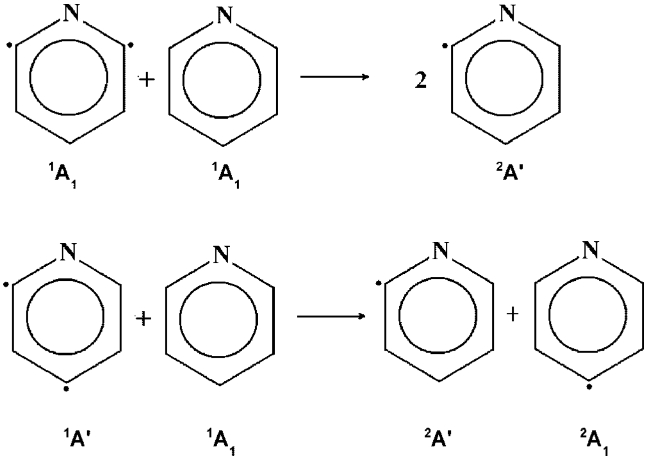

Figure 2. Pseudoisodesmic reactions defining diradical stabilization energies of the two didehydropyridine isomers.

reported for TDB indicates weak interactions of the third radical center with the *m*-benzyne diradical moiety, which is consistent with relatively strong bonding interactions between the radical centers in *m*-benzyne (the corresponding DSE is 16.7 kcal/mol). The sum of DSE of *m*-benzyne and TSE of TDB, a quantity characterizing interactions of all three radical centers, equals 19.5 kcal/mol.

Vertical and adiabatic energy gaps between different electronic states also reflect interactions between the unpaired electrons, e.g., bonding interactions stabilize low-spin states, whereas weakly interacting electrons may prefer high-spin coupling.

These interactions are sensitive to (and, therefore, may be tuned by) substituents and other chemical modifications, e.g., by introducing heteroatoms, allowing one to optimize desired chemical (reactivity) or physical (e.g., ground-state multiplicity) properties. These effects have been extensively explored[25−37] in diradicals.[38−41]

Owing to their open-shell character, triradicals are difficult to study both experimentally[22,42−44] and theoretically.[1,4,24,46−51] The studies of substituent effects in triradicals are relatively scarce.[45,48,52] The effect of substituents on electronic state ordering in the dehydrometaxylylene isomers has been investigated by Wang and Krylov.[48] Recently, Nash and co-workers reported experimental[45] and theoretical[52] studies of the tridehydropyridinium cations and compared their observations with the structural and thermochemical properties of isoelectronic tridehydrobenzenes. As in the diradicals,[25,35−37] introducing positive charge has been found to have a dramatic effect on the electronic structure of the triradicals;[45,48,52] however, the effects of heteroatoms have not yet been fully elucidated.

This paper investigates electronic structure of the two isoelectronic triradicals, TDB and TDP. We report equilibrium geometries of the three lowest electronic states, vertical and adiabatic states ordering and TSEs. The interactions between the radical centers are analyzed from two different perspectives, that is, considering the effect of heteroatom on TSE in TDP versus TDB, as well as the effect of adding a radical center to the parent diradical, 2,6-didehydropyridine (2,6-DDP) or 2,4-DDP. The differences between *m*-benzyne and the two DDP isomers are also briefly discussed.

2. Theoretical Methods and Computational Details

2.1. Triradicals and EOM-SF-CC Methods. Valid M_s = 1/2 and M_s = 3/2 wave functions that can be derived by distributing three electrons in three orbitals are shown in Figure 3. Whereas all doublets (c−j) and the low-spin component of quartet (b) are multiconfigurational, the high-spin (M_s = 3/2) component of the quartet state is singly determinantal. Moreover, all the low-spin determinants present in (b−j) are formally single spin-flipping excitations from the high-spin quartet determinant. This is exploited in the SF approach,[9−21] in which problematic low-spin states are described as spin-flipping, e.g., $\alpha \rightarrow \beta$, excitations from a high-spin reference state for which both dynamical and nondynamical correlation effects are much smaller than for the corresponding low-spin states. In the case of triradicals, we choose the high-spin (M_s = 3/2) component of the quartet state as a reference. The target states, the low-spin component of the quartet and the open- and closed-shell

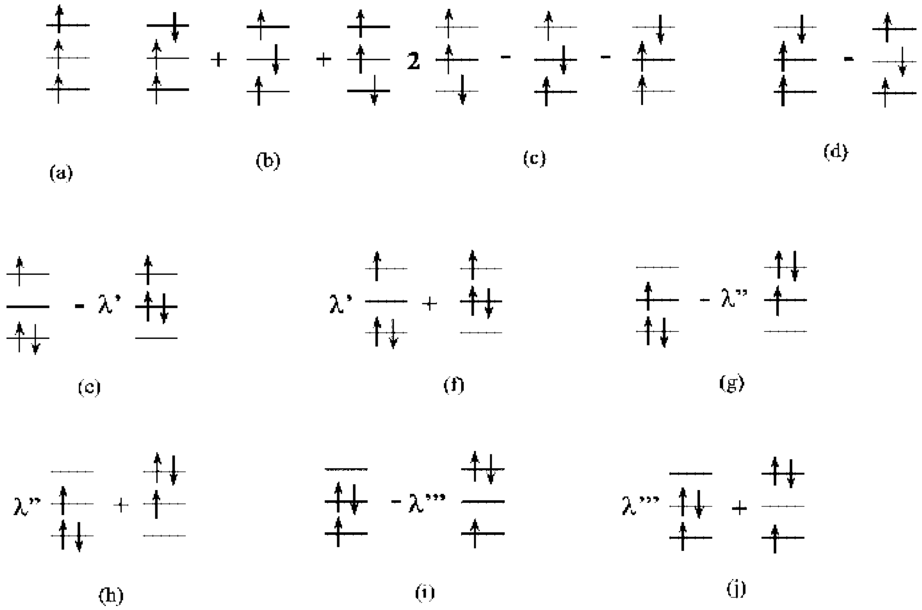

Figure 3. Wave functions that are eigenstates of $\hat{S}_z$ and $\hat{S}^2$, derived by distributing three electrons in three orbitals. Symmetry of the orbitals determines if these configurations can interact and further mix with each other. The coefficients λ depend on energy separation between the orbitals. All doublets (c−j) and the low-spin component of quartet (b) are multiconfigurational, whereas the high-spin component of quartet state (a) is singly determinantal. All the low-spin determinants present in (b−j) are formally single spin-flipping excitations from (a).

doublets ((b) and (c−j), respectively], are described as single electron excitations including the spin-flip of an electron

$$\Psi^{d,q}_{M_s=1/2} = \hat{R}_{M_s=-1}\tilde{\Psi}^{q}_{M_s=3/2} \tag{1}$$

where $\tilde{\Psi}^{q}_{M_s=3/2}$ is the ααα component of the quartet reference state ((a) from Figure 3), $\Psi^{d,q}_{M_s=1/2}$ stands for the final (M_s = 1/2) doublet and quartet states (b−j), and the operator $\hat{R}_{M_s=-1}$ is an excitation operator that flips the spin of an electron.

In the EOM-SF-CCSD model,[10] the reference wave function $\tilde{\Psi}^{q}_{M_s=3/2}$ is described by CCSD, and the operator $\hat{R}$ includes single and double excitations. The accuracy of EOM-SF-CCSD can be improved by perturbative account of triple excitations, e.g., by the EOM-SF-CCSD(fT) and EOM-SF-CCSD(dT) methods,[21] which are briefly described below.

In EOM-SF-CCSD(fT) and EOM-SF-CCSD(dT), the effect of triple excitations is described as perturbative correction to the EOM-CCSD energy. The perturbation theory is set up by taking the EOM-CCSD Hamiltonian, energies and wave functions as the zero-order quantities, H_0, $E^{(0)}$, and $\Psi^{(0)}$. In the O, S, and D blocks, H_0 is identical to the EOM-CCSD Hamiltonian matrix and in the T block it has only diagonal matrix elements

$$H_0 = \begin{bmatrix} \langle O|\bar{H}|O\rangle & \langle O|\bar{H}|S\rangle & \langle O|\bar{H}|D\rangle & \\ \langle S|\bar{H}|O\rangle & \langle S|\bar{H}|S\rangle & \langle S|\bar{H}|D\rangle & 0 \\ \langle D|\bar{H}|O\rangle & \langle D|\bar{H}|S\rangle & \langle D|\bar{H}|D\rangle & \\ & 0 & & \mathrm{Diag}^{TT} \end{bmatrix} \tag{2}$$

where $\bar{H} = \mathrm{e}^{-(\hat{T}_1+\hat{T}_2)}H\mathrm{e}^{(\hat{T}_1+\hat{T}_2)}$, and different choices of Diag^{TT} are described below. If T_1 and T_2 satisfy coupled-cluster equations for the reference, the $\langle S|\bar{H}|O\rangle$ and $\langle D|\bar{H}|O\rangle$ blocks vanish. For the SF variant, the $\langle O|\bar{H}|S\rangle$ and $\langle O|\bar{H}|D\rangle$ terms are also zero. The perturbation V is defined as $\bar{H} - H_0$. Second-order Rayleigh−Schrödinger perturbation theory gives the following expression for the energy correction

$$E^{(2)}_m = -\frac{1}{(3!)^2}\sum_{ijkabc}\frac{\tilde{\sigma}^{abc(m)}_{ijk}\sigma^{abc(m)}_{ijk}}{D^m_{ijkabc}} \tag{3}$$

where

$$\tilde{\sigma}^{abc(m)}_{ijk} = \langle\Phi_0 L^m_1|\bar{H}|\Phi^{abc}_{ijk}\rangle + \langle\Phi_0 L^m_2|\bar{H}|\Phi^{abc}_{ijk}\rangle \tag{4}$$

$$\sigma^{abc}_{ijk} = \langle\Phi^{abc}_{ijk}|\bar{H}|\Phi_0\rangle R^m_0 + \langle\Phi^{abc}_{ijk}|\bar{H}|R^m_1\Phi_0\rangle + \langle\Phi^{abc}_{ijk}|\bar{H}|R^m_2\Phi_0\rangle \tag{5}$$

$$D^m_{ijkabc} = \langle\Phi^{abc}_{ijk}|Diag^{TT}|\Phi^{abc}_{ijk}\rangle - E^{(CCSD)}_m \tag{6}$$

Two different choices of the diagonal, Diag^{TT}, define the EOM-CCSD(fT) and EOM-CCSD(dT) methods. The former uses Møller−Plesset type orbital energy differences, whereas the latter employs the full diagonal of $\bar{H}$

$$\langle\Phi_{ijk}|\mathrm{Diag}^{TT}|\Phi^{abc}_{ijk}\rangle = \langle\Phi^{abc}_{ijk}|\bar{H}|\Phi^{abc}_{ijk}\rangle \tag{7}$$

EOM-CCSD(dT) is slightly more accurate than EOM-CCSD(fT), at the expense of violating orbital invariance.[21]

2.2. Computational Details. The geometries of TDB, TDP, 2,6-DDP, and 2,4-DDP in different doublet and singlet electronic states were optimized using the 6-31G(d) basis set[53] and EOM-SF-CCSD[19] with the high-spin (quartet or triplet) UHF references. The structures of the quartet and triplet states, as well as doublet monoradicals (dehydropyridine, DP), were optimized using CCSD. All electrons were correlated in the geometry optimizations. Optimized geometries were used to compute vertical and adiabatic excitation energies.

Energy differences were computed using ROHF reference (to mitigate the effects of spin-contamination) with EOM-SF-CCSD, EOM-SF-CCSD(fT), and EOM-SF-CCSD(dT) and the cc-pVTZ basis set,[54] with six core orbitals being frozen.

The reactions defining TSEs of TDB and TDP are shown in Figure 1, and DSEs of the DDP diradicals are shown in Figure 2. TSEs and DSEs are computed using the procedure described in ref 24 via high-spin route to ensure balanced description of all the species

$$\mathrm{TSE} = \Delta E_{\mathrm{ls}} + \Delta\mathrm{ZPE} \tag{8}$$

where ZPE denotes zero-point vibrational energy, and the electronic energy differences are

$$\Delta E_{\mathrm{ls}} = \Delta E_{\mathrm{hs}} - \Delta DQ^{\mathrm{TDP}}_{\text{EOM-SF-CCSD(dT)}} + \Delta ST^{\mathrm{DDP}}_{\text{EOM-SF-CCSD(dT)}} \tag{9}$$

and ΔE_{hs} for the two reactions from Figure 1 are

$$\Delta E_{\mathrm{hs}} = E^{\text{2,6-DDP}}_{\mathrm{CCSD(dT)}}(^3B_2) + E^{\text{4-DP}}_{\mathrm{CCSD(dT)}}(^2A_1) - E^{\mathrm{TDP}}_{\mathrm{CCSD(dT)}}(^4B_2) - E^{\mathrm{pyridine}}_{\mathrm{CCSD(dT)}}(^1A_1) \tag{10}$$

$$\Delta E_{hs} = E^{\text{2,4-DDP}}_{\mathrm{CCSD(dT)}}(^3A') + E^{\text{2-DP}}_{\mathrm{CCSD(dT)}}(^2A') - E^{\mathrm{TDP}}_{\mathrm{CCSD(dT)}}(^4B_2) - E^{\mathrm{pyridine}}_{\mathrm{CCSD(dT)}}(^1A_1) \tag{11}$$

where ΔDQ^{TDP} and $\Delta ST^{\mathrm{DDP}}_{\text{EOM-SF-CCSD(dT)}}$ are the vertical quartet-doublet and singlet−triplet energy gaps of TDP and DDP, respectively, computed by EOM-SF-CCSD(dT). $E^{\text{2, 6-DDP}}_{\mathrm{CCSD(dT)}}(^3A_1)$, $E^{\text{2, 4-DDP}}_{\mathrm{CCSD(dT)}}(^3A')$, $E^{\text{4-DP}}_{\mathrm{CCSD(dT)}}(^2A_1)$, $E^{\text{2-DP}}_{\mathrm{CCSD(dT)}}(^2A')$, $E^{\mathrm{TDP}}_{\mathrm{CCSD(dT)}}(^4B_2)$, and $E^{\mathrm{pyridine}}_{\mathrm{CCSD(dT)}}(^1A_1)$ are the total CCSD(dT) energies of DDP, 4-DP, 2-DP, and TDB in the respective electronic states. All energies are computed at the optimized *ground-state* equilibrium geometries, using ROHF references for the high-spin states, and with core electrons frozen. ZPEs of all species were calculated by using harmonic frequencies computed by DFT with 50/50 exchange-correlation functional and the 6-31G(d) basis set.[53] For TDP in its ground ($^2B_2$) state, as well as the DDP isomers in their singlet states, we employed the SF-DFT method,[16] whereas regular Kohn−Sham DFT calculations were used for the rest of the species. The frequencies were computed at the respective optimized geometries. DFT frequencies and structures are given in Supporting Information.

We estimate the error bars of TSEs and DSEs computed by the above scheme[21,24] to be less than 1 kcal/mol.

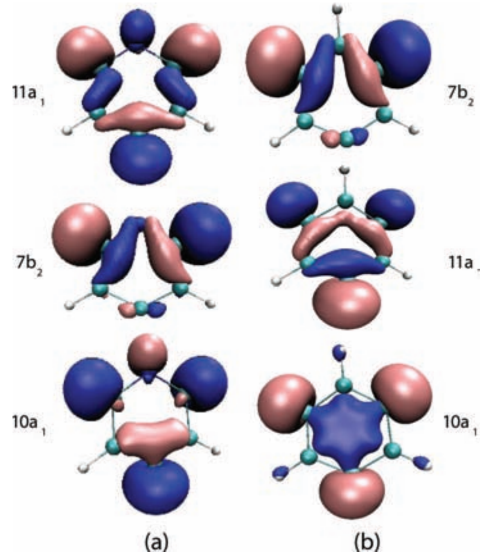

Figure 4. Frontier molecular orbitals of TDP (a) and TDB (b).

3. Results and Discussion

3.1. Molecular Orbitals Framework and Electronic Configurations of TBD, TDP, and DDP Isomers. Figure 4 presents the frontier molecular orbitals (MOs) of TDB and TDP. These orbitals derived from the three sp^2 hybridized orbitals at the radicals centers are $10a_1$, $11a_1$, and $7b_2$.

The $10a_1$ orbital, which is of bonding character between the three radical centers, is only slightly affected by the heteroatom, which reduces its bonding character. The $7b_2$ orbital is antibonding with respect to the C_3-C_5 and C_2-C_6 radical centers and nonbonding with respect to the third radical center. Whereas the heteroatom has a little influence on the shape of the $10a_1$ and $7b_2$ orbitals, the character of $11a_1$ is affected in a more significant way. In TDB, the $11a_1$ orbital is of bonding character with respect to the C_3-C_5 interactions. However, in TDP it acquires partially antibonding character with respect to the C_2 and C_4 radical centers. With respect to the third radical center, $11a_1$ is antibonding in both triradicals.

In the high-spin quartet state of the triradicals, all these orbitals are singly occupied. The two lowest doublet states have the following orbital occupancies:

$$^2A_1\text{: (core)}(10a_1)^2(11a_1)^1(7b_2)^0 \tag{12}$$

$$^2B_2\text{: (core)}(10a_1)^2(7b_2)^1(11a_1)^0 \tag{13}$$

Energetically, these orbitals lie between the bonding and antibonding π-orbitals. The π-systems of TDP and TDB are similar to those of pyridine and benzene, respectively. The relative energies of the frontier orbitals and, consequently, the electronic states ordering are rather sensitive to the geometry and also affected by the presence of the heteroatom. The $10a_1$ orbital is the lowest among the three. At the equilibrium geometry of the quartet state ($^4B_2$) of TDB, $10a_1$ is followed by $11a_1$ and $7b_2$, whereas this ordering between $11a_1$ and $7b_2$ orbitals is reversed in TDP. At the $^2B_2$ equilibrium geometries, $7b_2$ is below $11a_1$ in both triradicals; however, this ordering is reversed at the $^2A_1$ equilibrium geometries.

At the equilibrium geometries, the orbitals are well separated in energy and the lowest state is a doublet with the $10a_1$ orbital doubly occupied manifesting bonding interactions between the radical centers. TDB prefers $^2A_1$ ground state with the singly occupied $11a_1$ orbital and unoccupied $7b_2$, whereas TDP has $^2B_2$ ground state in which $7b_2$ is singly occupied, see eqs 12 and 13. This difference can be explained in terms of competition between two types of destabilizing interactions in TDP: the antibonding interactions of C_4 with C_2 and C_6 in the $^2A_1$ state and the antibonding interactions between C_2 and C_6 in the $^2B_2$ state. The former interactions appear to be stronger than the latter, thus resulting in the change of the ground-state character.

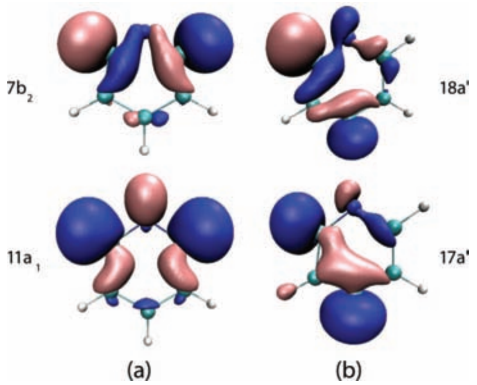

Figure 5. Frontier molecular orbitals of 2,6-DDP (a) and 2,4-DDP (b).

These bonding patterns are similar to those of the parent diradicals, 2,6-DDP, 2,4-DDP, and *m*-benzyne. The frontier MOs of the DDP isomers are shown in Figure 5. The MOs of 2,4-DDP resemble those of *m*-benzyne, whereas 2,6-DDP is more similar to TDB. The most important feature is that $11a_1$ acquires partial antibonding character between the radical centers. This results in destabilization of the singlet state and, consequently, reduces singlet−triplet gaps[26,28] in 2,6-DDP relative to 2,4-DDP and *m*-benzyne (see ref 55 for the compilation of theoretical and experimental studies on the DDP isomers) and very different DSEs, as discussed below.

The electronic configurations of the triplet states of 2,6-DDP and 2,4 DDP are

$$\text{(core)}(11a_1)^1(7b_2)^1 \tag{14}$$

$$\text{(core)}(17a')^1(18a')^1 \tag{15}$$

The two lowest singlet states of 2,6-DDP are of a closed-shell type and are dominated by configurations with either $11a_1$ or $7b_2$ being doubly occupied,[56] whereas the lowest singlet state of 2,4-DDP is more similar to that of *m*-benzyne and is dominated by the configuration in which bonding $17a'$ is doubly occupied.

3.2. Equilibrium Geometries. Equilibrium geometries of the low-lying electronic states of the triradicals are consistent with the electronic configurations and the associated MOs described above. The geometric parameters are summarized in Figures 6, and 7, and the Cartesian coordinates are given in Supporting Information.

In the quartet state, TDB has D_{3h} symmetry, at which the two doublet states form a degenerate Jahn−Teller pair.[47] Both $^2A_1$ and $^2B_2$ undergo distortions to C_{2v}, the former state being a minimum and the latter a transition state along the pseudorotation coordinate. The two structures feature shorter C_1-C_3 distances relative to the quartet state. The C_3-C_5 distance

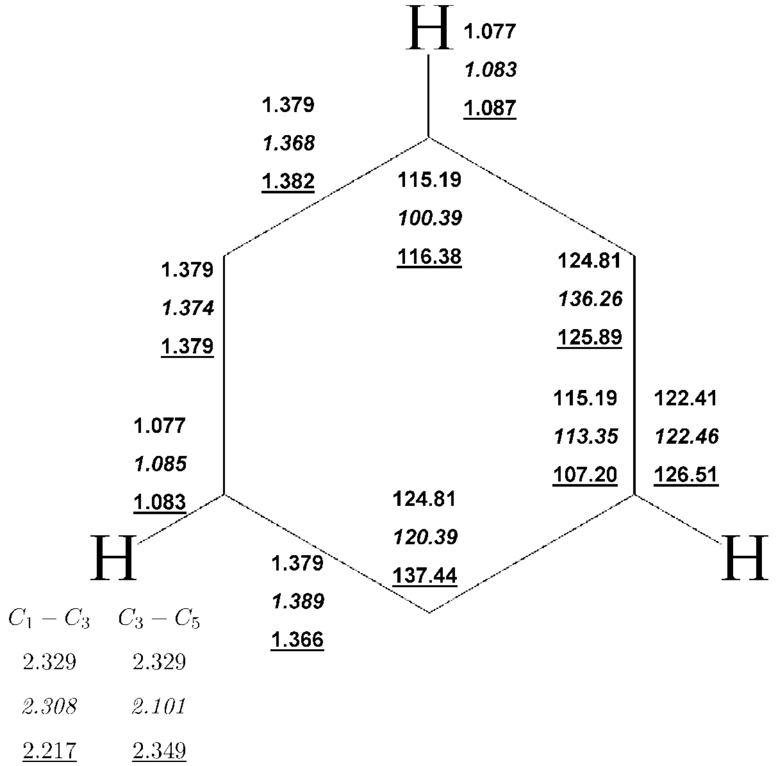

Figure 6. Geometric parameters of 1,3,5-tridehydrobenzene. The values from top to bottom correspond to the $^4B_2$, $^2A_1$, and $^2B_2$ states, respectively.

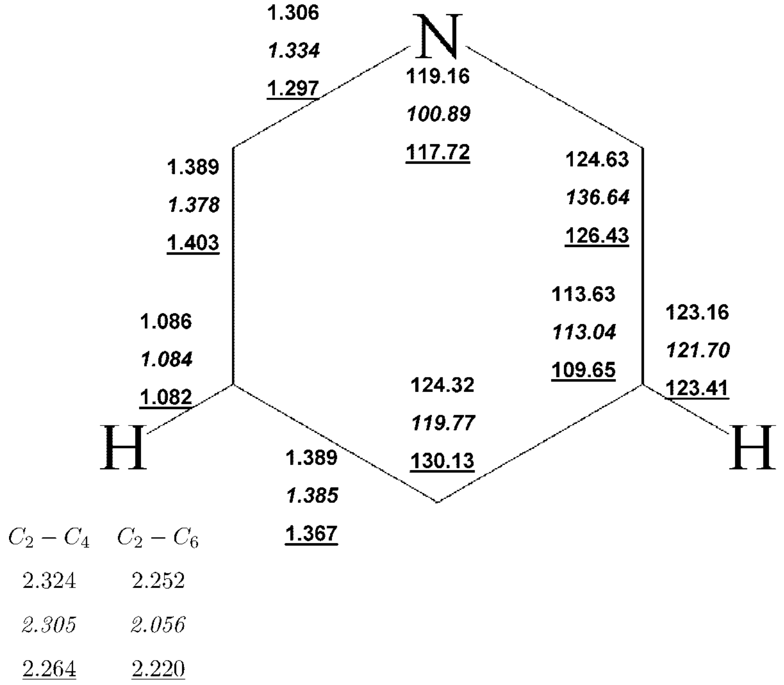

Figure 7. Geometric parameters of 2,4,6-tridehydropyridine. The values from top to bottom correspond to the $^4B_2$, $^2A_1$, and $^2B_2$ states, respectively.

increases in the $^2B_2$ state relative to the quartet state by about 0.02 Å, whereas it is contracted by 0.2 Å in the $^2A_1$ state due to the bonding interactions between the radical centers.

Contrary to TDB, both doublets of TDP are local minima, as confirmed by frequency calculations. In both doublet states, the C_2-C_6 and C_2-C_4 distances are shorter relative to the quartet state. For the $^2A_1$ state, these differences are 0.2 and 0.02 Å, respectively, whereas in the $^2B_2$ state, these differences are 0.03 and 0.06 Å, respectively.

Figures 8 and 9 present the geometric parameters of the DDP isomers in the relevant electronic states. In 2,6-DDP, the C_2-C_6 distance is shortened in the lower $^1A_1$ state by 0.15 Å relative to the triplet state, which is a signature of the bonding interactions between the radical centers. In the second $^1A_1$ state,

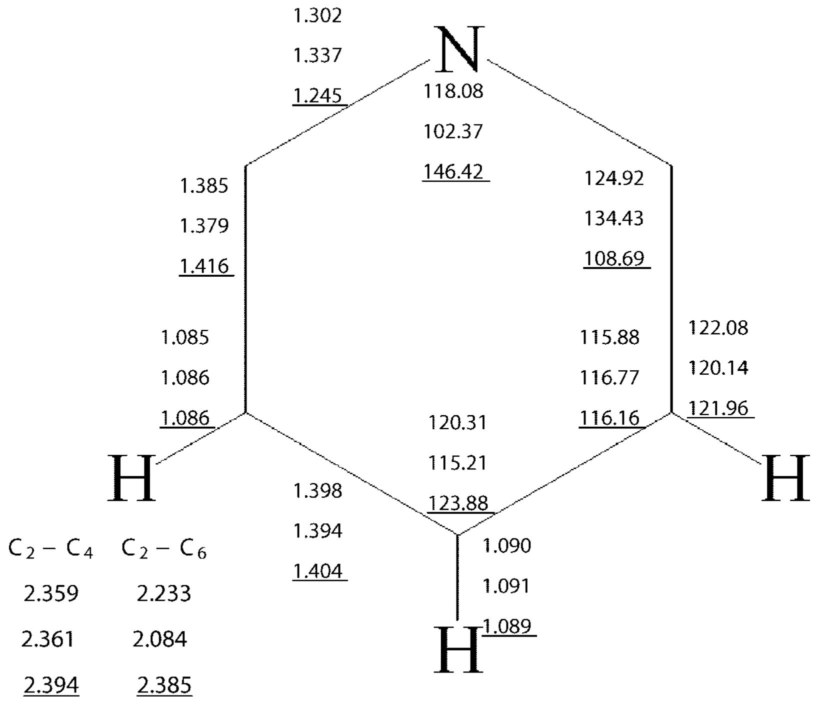

Figure 8. Geometric parameters of 2,6-didehydropyridine. The values from top to bottom correspond to the $^3B_2$, 1^1A_1, and 2^1A_1 states, respectively.

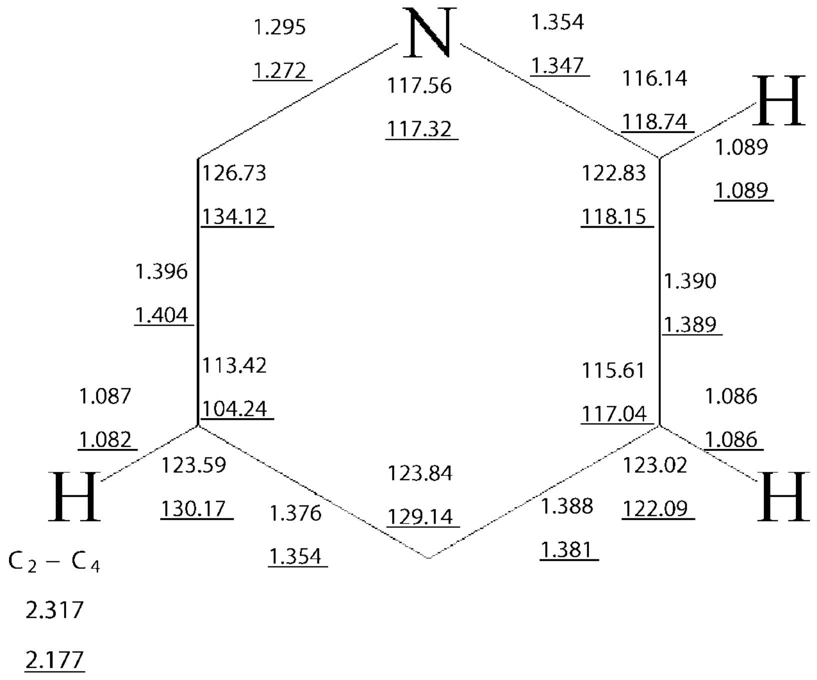

Figure 9. Geometric parameters of 2,4-didehydropyridine. The values from top to bottom correspond to the $^3A'$ and $^1A'$ states, respectively.

TABLE 1: 2,4,6-Tridehydropyridine: Total Energy (hartree) for the Ground ($^2B_2$) State and Vertical and Adiabatic Excitation Energies (eV) of the $^2A_1$ and $^4B_2$ States Using the EOM-SF Methods and the cc-pVTZ Basis Set[a]

Method	$E_{\mathrm{tot}}(^2B_2)$	ΔE^{v}_{12}	ΔE^{v}_{13}	ΔE^{v}_{21}	ΔE^{v}_{23}	ΔE^{a}_{12}	ΔE^{a}_{13}	ΔE^{a}_{23}
CCSD	−245.75933	0.979	1.207	−0.006	1.040	0.651	1.106	0.456
CCSD(fT)	−245.76823	1.011	1.307	0.033	1.177	0.625	1.205	0.580
CCSD(dT)	−245.76961	1.016	1.325	0.045	1.209	0.613	1.223	0.610

[a] The superscripts 1, 2, and 3 correspond to the $^2B_2$, $^2A_1$, and $^4B_2$ states, respectively.

the radical centers move further apart by 0.15 Å relative to the triplet state, indicating antibonding interactions. In 2,4-DDP, the radical centers C_2 and C_4 are closer than in its triplet state by 0.14 Å and the C_2−C_3−C_4 angle reduces by about 9° indicating bonding interactions in the singlet state. This is similar to the *m*-benzyne structure, in which the distance between the radical centers is contracted by 0.3 Å and the C_1−C_2−C_3 angle is reduced by 18°.[17]

TABLE 2: 1,3,5-Tridehydrobenzene: Total Energy (hartree) for the Ground ($^2A_1$) State and Vertical and Adiabatic Excitation Energies (eV) of the $^2B_2$ and $^4B_2$ States Using the EOM-SF Methods and the cc-pVTZ Basis Set[a]

method	$E_{tot}(^2A_1)$	ΔE^v_{12}	ΔE^v_{13}	ΔE^v_{21}	ΔE^v_{23}	ΔE^a_{12}	ΔE^a_{13}	ΔE^a_{23}
CCSD	−229.71983	0.905	1.762	0.509	1.446	0.010	0.237	0.227
CCSD(fT)	−229.72873	0.947	1.893	0.541	1.572	0.017	0.273	0.256
CCSD(dT)	−229.73016	0.954	1.918	0.549	1.598	0.016	0.277	0.262

[a] The superscripts 1, 2, and 3 correspond to the $^2A_1$, $^2B_2$, and $^4B_2$ states, respectively.

TABLE 3: 2,6-Didehydropyridine: Total Energy (hartree) for the Ground (1^1A_1) State and Vertical and Adiabatic Excitation Energies (eV) of the 2^1A_1 and $^3B_2$ States Using the EOM-SF Methods and the cc-pVTZ Basis Set[a]

method	$E_{tot}(1^1A_1)$	ΔE^v_{13}	ΔE^v_{23}	ΔE^a_{12}	ΔE^a_{13}	ΔE^a_{23}
CCSD	−246.41510	0.386	1.027	0.132	−0.037	−0.169
CCSD(fT)	−246.42244	0.431	1.114	0.042	−0.007	−0.049
CCSD(dT)	−246.42355	0.440	1.126	0.033	0.001	−0.032

[a] The superscripts 1, 2, and 3 correspond to the 1^1A_1, 2^1A_1, and $^3B_2$ states, respectively.

TABLE 4: 2,4,6-Tridehydropyridine Triradical Stabilization Energy (kcal/mol) and the Individual Contributions (see text)[a]

radical center	ΔE_{hs}	ΔDQ^{TDP}	ΔST^{DDP}	ΔE_{ls}	ΔZPE	TSE
C_4	−0.095	−30.561	−10.147	20.319	−0.583	19.736
C_2	−0.381	−30.561	−30.019	0.161	−0.369	−0.208

[a] The EOM-SF-CCSD(dT) values of ΔDQ and ΔST are used.

TABLE 5: Diradical Stabilization Energies (kcal/mol) of the DDP Isomers and the Individual Contributions (see text)[a]

molecule	ΔE_{hs}	ΔST^{DDP}	ΔE_{ls}	ΔZPE	DSE
2,6-DDP	−10.686	−10.147	−0.539	0.861	0.322
2,4-DDP	−10.400	−30.019	19.619	0.694	20.313

[a] The EOM-SF-CCSD(dT) value of ΔST is used.

Thus, the addition of the third radical center in 2,6-DDP affects the balance between bonding and antibonding interactions and stabilizes the doublet state.

3.3. Vertical and Adiabatic Excitation Energies. This section presents the electronic state ordering in TDP, TDB, and two DDP isomers. Figure 10 gives a qualitative picture of the electronic state ordering and defines important energy differences. In the discussion below, state 1 refers to the EOM-SF-CCSD(dT) ground state, and the relative energies of other states relative to each other are defined as in Figure 10. The notation ΔE_{ij} denotes energy difference between the *i*th and the *j*th states: $\Delta E_{ij} = E_j - E_i$. The ground states of TDP and TDB are $^2B_2$ and $^2A_1$, respectively. EOM-SF-CCSD predicts a triplet ground state of 2,6-DDP, but EOM-SF-CCSD(dT) favors a singlet ground state; hence, the relative energies of the electronic states of 2,6-DDP are tabulated with respect to the singlet state. Note that the computed adiabatic gap between the singlet and the triplet is too small to be resolved with present methodology. Using these notations, the total ground-state energies and the vertical and adiabatic gaps between the electronic states of TDP, TDB, and 2,6-DDP are summarized in Tables 1, 2, and 3, respectively.

As discussed above, both triradicals prefer low-spin ground states; however, the character of the lowest doublet changes in TDB as compared to TDP. The former has $^2A_1$ ground state, and the latter has $^2B_2$ ground state. The doublet states of TDB are subject of the Jahn−Teller effect resulting in very small adiabatic energy difference (without ZPE), i.e., 0.02 eV (0.37 kcal/mol). On the other hand, the perturbation due to the presence of the N atom being quite prominent, this adiabatic energy difference is as high as 0.61 eV (14 kcal/mol) in TDP, and the doublet-quartet gap is 1.22 eV (28 kcal/mol).

In the 2,6-DDP diradical, the presence of nitrogen has a dramatic effect on the relative energies of the triplet and singlet states resulting in destabilization of the singlet state and reducing the singlet−triplet gap to nearly zero,[26,28] relative to 0.9 eV in *m*-benzyne.[21] Note that EOM-SF-CCSD and EOM-SF-CCSD(fT) favor triplet ground state; however, EOM-SF-CCSD(dT) predicts the singlet ground state. Our best estimate of the adiabatic energy difference (0.049 and 0.001 eV with and without ZPE contributions, respectively) is beyond the resolution of the present methodology. The ST gaps in 2,4-DDP are much larger. The EOM-SF-CCSD(dT) values for vertical and adiabatic ST gaps are 1.302 and 1.065 eV, respectively.

Thus, adding the third radical center at the C_4 position in DDP stabilizes the low-spin state by strong singlet couplings between C_2/C_4 and C_2/C_6.

Quantitatively, the effect of triples correction is not very large and increases vertical excitation energies between the two

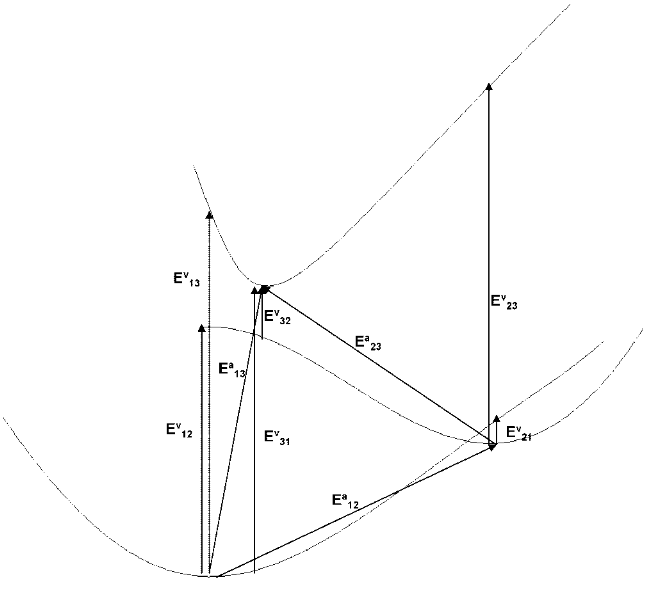

Figure 10. Vertical and adiabatic electronic states ordering defining the important energy differences.

doublet states of TDP and TDB by 0.04−0.05 eV. The vertical doublet−quartet gaps increase by 0.1−0.2 eV upon inclusion of triples. In 2,6-DDP, the vertical singlet−triplet gap increases by 0.06−0.1 eV, similarly to *m*-benzyne.[21] The (fT) correction reduces the adiabatic gap by 0.03 eV, and (dT) reduces it further by 0.01 eV predicting the singlet ground state.

3.4. Triradical Stabilization Energies. The reactions defining TSEs of TDB and TDP are shown in Figure 1, and those defining relevant DSEs are shown in Figure 2. The quantities used to compute TSEs of TDP by eqs 8 and 10, as well as resulting TSEs, are presented in Table 4.

TSE corresponding to the separation of the C_4 radical center in TDP equals 19.7 kcal/mol, which is much larger compared to that of TDB (2.8 kcal/mol from ref 24). However, TSE corresponding to the separation of C_2 is essentially zero. This is consistent with the MOs and energy gaps discussed above: the presence of nitrogen breaks the interactions between C_2 and C_6, which makes each of these centers available for bonding interactions with C_4. In contrast, in TDB, the C_1 and C_3 radical centers interact much stronger, similarly to *m*-benzyne, and addition of the third center has little effect, just like addition of the radical center at C_2 to 2,4-DDP.

The DSEs of the DDP isomers (given in Table 5) confirm similar bonding patterns: the interaction between radical centers in 2,6-DDP is essentially zero (DSE = 0.3 kcal/mol), in stark contrast to DSE in 2,4-DDP of 20.3 kcal/mol, which is close to 16.7 kcal/mol DSE of *m*-benzyne. Our DSEs are in agreement with previously reported CCSD(T) values.[26]

Another interesting quantity is the sum of TSE and DSE of the target diradical. This value quantifies interactions between all three radical centers and is invariant to the choice of the TSE definition (e.g., C_4 or C_2). In TDB, this value is 19.5 kcal/mol, and in TDP, it is 20.1 kcal/mol. Thus, although the presence of the heteroatom changes the bonding patterns between the radical centers, it has negligible effect on total stabilization energy.

The analysis of the individual contributions from Table 4 offers additional insight. The contribution of zero-point energies is small, i.e., their difference is less than 1 kcal/mol. The major contribution to TSE is from the doublet−quartet and singlet−triplet energy gaps in the tri- and diradicals, respectively, and ΔE_{hs}. As expected for the three same-spin electrons, ΔE_{hs} is very small, i.e., −0.095 kcal/mol in TDP. In the case of TDB, this value is larger and equals −6.15 kcal/mol. The vertical doublet−quartet gaps in TDP and TDB are comparable. However, the corresponding singlet−triplet gap is much smaller in 2,6-DDP (0.44 eV), as compared to the one in *m*-benzyne[21] (0.89 eV), or in 2,4-DDP. Moreover, the 2-pyridinyl radical lies lower in energy than the 4-pyridinyl radical by 0.20 eV (4.59 kcal/mol) as calculated by the CCSD(dT) method. All these factors result in large TSE corresponding to C_4 and very small TSE corresponding to C_2.

4. Conclusions

This paper presents theoretical predictions for the equilibrium geometries, electronic states ordering, and TSEs in TDP. It also investigates bonding patterns between the unpaired electrons and compares them to TDB. In addition, the related diradicals, *m*-benzyne, 2,6-DDP, and 2,4-DDP are compared.

The most important effect of the nitrogen atom is that it introduces antibonding interactions between the C_2 and C_6 radical centers in TDP and 2,6-DDP, which changes bonding patterns in these species as compared to TDB and *m*-benzyne.

Whereas *m*-benzyne and 2,4-DDP prefer singlet ground state, the antibonding interactions in the lowest singlet state of 2,6-DDP destabilizes the singlet resulting in nearly degenerate singlet and triplet states. Addition of the radical center, at the para-position stabilizes the low-spin states and results in shorter distances between the radical centers.

The presence of the heteroatom results in the increased stabilizing interactions between C_4 and C_2/C_6, as manifested by the respective TSEs. TSEs corresponding to the separation of C_4 and C_2 are 19.7 and −0.2 kcal/mol, respectively, in contrast to 2.8 kcal/mol in TDB. The total interaction energy of the three radical centers is very similar in both triradicals and is 19.5 and 20.1 kcal/mol in TDB and TDP, respectively.

Acknowledgment. This work was conducted under the auspices of the *iOpenShell* Center for Computational Studies of Electronic Structure and Spectroscopy of Open-Shell and Electronically Excited Species (iopenshell.usc.edu) supported by the National Science Foundation through the CRIF:CRF Grant Nos. CHE-0625419, 0624602, and 0625237. We also gratefully acknowledge support of the National Science Foundation through the Grant No. CHE-0616271.

Supporting Information Available: DFT frequencies and structures and Cartesian coordinates. This material is available free of charge via the Internet at http://pubs.acs.org.

References and Notes

(1) Krylov, A. I. *J. Phys. Chem. A* **2005**, *109*, 10638.

(2) *Magnetic properties of organic materials*; Lahti, P. M., Ed.; Marcel Dekker, Inc.: New York, 1999.

(3) Rajca, A. *Chem. Rev.* **1994**, *94*, 871.

(4) Prasad, B. L. V.; Radhakrishnan, T. P. *J. Phys. Chem. A* **1997**, *101*, 2973.

(5) Selby, T. D.; Stickley, K. R.; Blackstock, S. C. *Org. Lett.* **2000**, *2*, 171.

(6) Sato, K.; Yano, M.; Furuichi, M.; Shiomi, D.; Takui, T.; Abe, K.; Itoh, K.; Higuchi, A.; Katsuma, K.; Shirota, Y. *J. Am. Chem. Soc.* **1997**, *119*, 6607.

(7) Weyland, T.; Costuas, K.; Mari, A.; Halet, J.; Lapinte, C. *Organometallics* **1998**, *17*, 5569.

(8) Hosokoshi, Y.; Katoh, K.; Nakazawa, Y.; Nakano, H.; Inoue, K. *J. Am. Chem. Soc.* **2001**, *123*, 7921.

(9) Krylov, A. I. *Chem. Phys. Lett.* **2001**, *338*, 375.

(10) Levchenko, S. V.; Krylov, A. I. *J. Chem. Phys.* **2004**, *120*, 175.

(11) Krylov, A. I. *Acc. Chem. Res.* **2006**, *39*, 83.

(12) Krylov, A. I.; Sherrill, C. D. *J. Chem. Phys.* **2002**, *116*, 3194.

(13) Krylov, A. I. *Chem. Phys. Lett.* **2001**, *350*, 522.

(14) Sears, J. S.; Sherrill, C. D.; Krylov, A. I. *J. Chem. Phys.* **2003**, *118*, 9084.

(15) Casanova, D.; Head-Gordon, M. *J. Chem. Phys.* **2008**, *129*, 064104.

(16) Shao, Y.; Head-Gordon, M.; Krylov, A. I. *J. Chem. Phys.* **2003**, *118*, 4807.

(17) Slipchenko, L. V.; Krylov, A. I. *J. Chem. Phys.* **2002**, *117*, 4694.

(18) Kus, T.; Bartlett, R. J. *J. Chem. Phys.* **2008**, *129*, 104301.

(19) Levchenko, S. V.; Wang, T.; Krylov, A. I. *J. Chem. Phys.* **2005**, *122*, 224106.

(20) Slipchenko, L. V.; Krylov, A. I. *J. Chem. Phys.* **2005**, *123*, 084107.

(21) Manohar, P. U.; Krylov, A. I. *J. Chem. Phys.* **2008**, *129*, 194105.

(22) Lardin, H. A.; Nash, J. J.; Wenthold, P. G. *J. Am. Chem. Soc.* **2002**, *124*, 12612.

(23) Wierschke, S. G.; Nash, J. J.; Squires, R. R. *J. Am. Chem. Soc.* **1993**, *115*, 11958.

(24) Cristian, A. M. C.; Shao, Y.; Krylov, A. I. *J. Phys. Chem. A* **2004**, *108*, 6581.

(25) West, A.P. Jr.; Silverman, S. K.; Dougherty, D. A. *J. Am. Chem. Soc.* **1996**, *118*, 1452.

(26) Cramer, C. J.; Debbert, S. *Chem. Phys. Lett.* **1998**, *287*, 320.

(27) Cramer, C. J. *J. Am. Chem. Soc.* **1998**, *120*, 6261.

(28) Cramer, C. J.; Debbert, S. L. *ijmspect* **2000**, *201*, 1.

(29) Clark, A. E.; Davidson, E. R. *J. Org. Chem.* **2003**, *68*, 3387.

(30) Berson, J. A. In *Magnetic properties of organic materials*; Lahti, P. M., Ed.; Marcel Dekker, Inc.: New York, 1999; pp 7−26.

(31) Bush, L. C.; Heath, R. B.; Feng, X. W.; Wang, P. A.; Maksimovic, L.; Song, A. I.; Chung, W. S.; Berinstain, A. B.; Scaiano, J. C.; Berson, J. A. *J. Am. Chem. Soc.* **1997**, *119*, 1406.

(32) Ito, A.; Ino, H.; Ichiki, H.; Tanaka, K. *J. Phys. Chem. A* **2002**, *106*, 8716.

(33) Geise, C. M.; Hadad, C. M. *J. Org. Chem.* **2000**, *65*, 8348.

(34) Shultz, D. A.; Bodnar, S. H.; Lee, H.; Kampf, J. W.; Incarvito, C. D.; Rheingold, A. L. *J. Am. Chem. Soc.* **2002**, *124*, 10054.

(35) Nelson, E. D.; Thoen, K. K.; Kenttamaa, H. I. *J. Am. Chem. Soc.* **1998**, *120*, 3792.

(36) Tichy, S. E.; Nelson, E. D.; Amegayibor, F. S.; Kenttamaa, H. I. *J. Am. Chem. Soc.* **2004**, *126*, 12957.

(37) Wang, T.; Krylov, A. I. *J. Chem. Phys.* **2005**, *123*, 104304.

(38) Salem, L.; Rowland, C. *Angew. Chem., Int. Ed. Engl.* **1972**, *11*, 92.

(39) *Diradicals*; Borden, W. T., Ed.; Wiley: New York, 1982.

(40) Bonačić-Koutecký, V.; Koutecký, J.; Michl, J. *Angew. Chem., Int. Ed. Engl.* **1987**, *26*, 170.

(41) Michl, J. *J. Mol. Struct. THEOCHEM* **1992**, *260*, 299.

(42) Slipchenko, L. V.; Munsch, T. E.; Wenthold, P. G.; Krylov, A. I. *Angew. Chem., Int. Ed.* **2004**, *43*, 742.

(43) Venkataramani, S.; Winkler, M.; Sander, W. *Angew. Chem., Int. Ed.* **2005**, *44*, 6306.

(44) Venkataramani, S.; Winkler, M.; Sander, W. *Angew. Chem., Int. Ed.* **2007**, *46*, 4888.

(45) Jankiewicz, B. J.; Adeuya, A.; Yurkovich, M. J.; Vinueza, N. R.; Gardner, S. J.; Zhou, M.; Nash, J. J.; Kenttämaa, H. I. *Angew. Chem., Int. Ed.* **2007**, *46*, 9198.

(46) Bettinger, H. F.; Schleyer, P.v.R.; Schaefer, H. F., III *J. Am. Chem. Soc.* **1999**, *121*, 2829.

(47) Slipchenko, L. V.; Krylov, A. I. *J. Chem. Phys.* **2003**, *118*, 9614.

(48) Wang, T.; Krylov, A. I. *Chem. Phys. Lett.* **2006**, *426*, 196.

(49) Koziol, L.; Winkler, M.; Houk, K. N.; Venkataramani, S.; Sander, W.; Krylov, A. I. *J. Phys. Chem. A* **2007**, *111*, 5071.

(50) Nguyen, H. M. T.; Gopakumar, G.; Peeters, J.; Nguyen, M. T. *J. Chem. Phys.* **2004**, *108*, 8411.

(51) Nguyen, H. M. T.; Holtzl, T.; Gopakumar, G.; Veszpremi, T.; Peeters, J.; Nguyen, M. T. *Chem. Phys.* **2005**, *316*, 125.

(52) Nash, J. J.; Kenttämaa, H. I.; Cramer, C. J. *J. Phys. Chem. A* **2008**, *112*, 5542.

(53) Hariharan, P. C.; Pople, J. A. *Theor. Chim. Acta* **1973**, *28*, 213.

(54) Dunning, T. H. *J. Chem. Phys.* **1989**, *90*, 1007.

(55) Cioslowski, J.; Szarecka, A.; Moncrieff, D. *Mol. Phys.* **2003**, *101*, 839.

(56) Winkler, M.; Koziol, L.; Krylov, A. I. In preparation.

JP810522E